Biodistribution and In Vivo Kinetics of Iodine-131 Lipiodol Infused via the Hepatic Artery of Patients with Hepatic Cancer

Masayuki Nakajo, Hisashi Kobayashi, Kunisada Shimabukuro, Kazuo Shirono, Hiromichi Sakata, Masato Taguchi, Noriaki Uchiyama, Toshihide Sonoda, and Shinji Shinohara

Department of Radiology, Faculty of Medicine, Kagoshima University, Japan

The biodistribution and in vivo kinetics of [^{131}I]lipiodol infused into the hepatic artery were studied to estimate the potential of internal radiotherapy of hepatic cancer in five patients. It accumulated only in the vascular tumors and adjacent hepatic tissue (AHT) supplied by the infused artery, and to a lesser extent in the lung throughout 8 days imaging sequence. Iodine-131 lipiodol appeared to lead to oil embolization of the tumor and AHT followed by secondary embolization to the lungs and finally the activity was mainly excreted into urine. Four tumors had rapidly and slowly decreasing components, while the AHT activity decreased exponentially from the beginning. The effective half life in tumors was longer with the slow component (mean ± s.d.: 5.7 ± 1.2 days) than the AHT (3.7 ± 0.6 days). The tumor/AHT concentration ratio in three patients at 2 hr was estimated to be 7.5–21. The activity was lower in the lungs than in the AHT in four patients. Iodine-131 lipiodol thus may be used as an intra-arterial infusion agent to treat certain vascular hepatic cancers.

J Nucl Med 29:1066–1077, 1988

Lipiodol (lipiodol ultra fluid, ethiodol, ethyl esters of the fatty acid of poppyseed oil: 38% iodine by weight) (A product of Andre-Gelbe Laboratories, France, obtained through Kodama Co., Ltd., Tokyo, Japan.) was found to be selectively retained in the tumor vessels of hepatoma when infused into the hepatic artery (*1*). In Japan, this iodized oil has been increasingly used intra-arterially for the detection of primary and metastatic liver cancer (*2–4*) and for the treatment of hepatoma as lipid-chemotherapeutic mixtures (*5,6*). However, its biodistribution and in vivo kinetics when infused into the hepatic artery have not been fully elucidated. The phenomenon of selective retention in the hepatoma and iodine content of lipiodol suggest the potential of internal radiotherapy of hepatic neoplasm by transcatheter intra-hepatic arterial infusion of iodine-131- (^{131}I) labeled lipiodol.

This study was designed to elucidate the biodistribution and in vivo kinetics of [^{131}I]lipiodol and thereby to estimate the potential for internal radiotherapy of hepatoma by transcatheter intra-arterial infusion of [^{131}I]lipiodol.

Received Sept. 2, 1987; revision accepted Dec. 1, 1987

For reprints and correspondence contact: M. Nakajo, MD, Dept. of Radiology, Faculty of Medicine, Kagoshima University, 1208-1 Usuki-cho, Kagoshima-shi, Kagoshima 890, Japan

MATERIALS AND METHODS

Iodine-131 Lipiodol

Iodine-131 lipiodol was obtained from a commercial laboratory (Daiichi Radioisotope Laboratories, Ltd., Tokyo, Japan). It was prepared at a specific concentration of 3.3 mCi/ml and specific activity of 2.6 mCi/g with radiochemical purity of 96% using an iodide exchanging technique (*7*).

Patients

Four patients with hepatoma and one with cholangiocarcinoma were included in this study after obtaining informed consent. The diagnosis was made by liver biopsy, angiography, TCT examination, measurement of serum alpha-fetoprotein and clinical course. The main findings in the hepatic arteriograms included hyperneovascularity and tumor stain in the four hepatomas and marginal irregularity of the arterial branches with little tumor stain in the cholangiocarcinoma (Table 1).

Iodine-131 Lipiodol Infusion Method

Three hundred milligrams of potassium iodide a day were given orally to block uptake of ^{131}I by the thyroid glands on the day before infusion of the tracer and for 6 days afterwards.

TABLE 1
List of Patients, Tumor Characteristics and I-131 Lipiodol Infused Artery

Patient no.	Age/sex (yr)	Tumor					[^{131}I]lipiodol infused artery
				Angiographic finding		Size (cm) In TCT	
		Diagnosis	Location	Vascularity	Stain		
1	67/F	Hepatoma	Segment 8	+	+	3.0 × 3.2	RHA
2	47/M	Hepatoma	Segment 6	+	+	3.0 × 4.0	PHA
3	64/F	Hepatoma	Segment 8	+	+	3.6 × 3.6	RHA
4	55/M	Hepatoma	Segment 3,4	+	+	12.0 × 11.5	LHA
5	70/F	Cholangiocarcinoma	Segment 3	−	−	6.5 × 4.0	PHA

The patient was positioned supine between the dual detectors of a rotating scintillation camera (ZLC-75: Siemens Gammasonics, Inc., Des Plaines, IL) with medium-energy multiparallel hole collimators. A volume of 5 ml of [^{131}I]lipiodol mixed with lipiodol (480-550 μCi/patient) was slowly infused at a rate of 1 ml/min into the proper (PHA), right (RHA) or left hepatic artery (LHA) supplying the tumor by Seldinger's technique. This was followed by infusion of physiological saline solution to clear the tracer in the catheter.

Imaging and data collection: As soon as the tracer infusion started, an anterior dynamic data acquisition over the liver was made for 10 min with every 30 sec using a nuclear medicine minicomputer (SCINTIPAC-2400, Shimazu Co., Ltd., Kyoto, Japan) attached to the gamma camera. Five-min planar images and data over the liver were acquired at 30 min and almost daily until 8 days. Whole body images were obtained at 1 hr, and every other day until 8 days. Single photon emission computed tomography (SPECT) data acquisition was made with 36 projections and 90 sec acquisition time for each projection at 2 hr and 1, 3 and 7 days. The energy window was 20% centered on the 364 keV energy emission of ^{131}I.

Estimation of biodistribution and in vivo kinetics: Biodistribution of the tracer was assessed visually in the serially obtained analog images. Before processing human data for quantitative analysis, liver phantom studies were performed to examine whether the changes in counts of the region of interest (ROI) in the same position in the serial digital planar and SPECT images reflected those in absolute activity. The liver phantom and normal torso (products of Kyoto Scientific Specimen Co., Ltd., Kyoto, Japan) had 1,750 ml and 11.5 l in volume, respectively. On each occasion the liver phantom was filled with homogeneous solution containing ^{131}I at various concentrations (0, 0.025, 0.05, and 0.25 μCi), it was suspended in the torso which was filled with water. Planar and SPECT data acquisition were performed using the same conditions as in the human study. A 9-point smoothing was performed for planar data processing. Two 25-point smoothings and 0.05 absorption correction coefficient were used for SPECT data processing. These processing factors were determined by examination of the homogeneity of the digital images. Small and large rectangular regions of interest (ROIs) were set over the same position of the liver phantom in the serial planar and SPECT digital images.

We confirmed a very high linear correlation between absolute ^{131}I concentration (Y) and ROI counts (X) in both planar and SPECT images: $Y = 1.02X - 0.02$ ($r = 0.9996$) for 25 pixel ROI and $Y = 0.98X + 0.01$ ($r = 0.9996$) for 315 pixel ROI in the planar imaging; $Y = 0.99X + 0.02$ ($r = 0.9993$) for 25 pixel ROI and $Y = 0.99X + 0.01$ for 231 pixel ROI ($r = 0.9998$) in the SPECT imaging. These experimental results indicate that serial changes of ROI counts in the same position in both planar and SPECT digital images reflect correctly those in absolute activity. Therefore the human data were processed by the same techniques that had been employed in the phantom study.

For the assessment of the tracer flow during the initial 10 min, the time-activity curves over the tumor, adjacent hepatic tissue (AHT) and lung were generated by setting rectangular ROIs (49 pixels) over them after performing a 9-point smoothing.

Rectangular ROIs were also set over the liver as a whole as the size of visible liver including the tumor and AHT, and over the left middle lung (49 pixels) respectively in the 30 min anterior chest-abdominal image in each patient to obtain the daily time-activity relationships over these regions. The size and position of the ROIs in the subsequent images were the same as those used in the 30-min images.

In order to obtain separate time-activity relationships over the tumor and AHT, rectangular ROIs (25 pixels) were set over them in the 2-hr SPECT image which contained the maximum counts of the tumor in all slices except for Patient 5. The tumor of Patient 5 showed a photon deficient area. The SPECT image which crossed its mid-portion, therefore, was selected for the ROI setting. The mean counts/pixel of ROIs over the visible liver in the 30-min anterior chest-abdominal image and over the tumor in the 2-hr SPECT image were regarded as 100, respectively. For Patient 5 whose tumor showed little specific uptake, the mean counts/pixel of the ROI over the AHT in the 2-hr SPECT image was regarded as 100. The relative activity versus time relationship was plotted on a semilogarithmic graph paper.

Venous blood was obtained serially at 5, 15, and 30 min and at 1, 2, 4 and every 24 hr until 8 days to assess the blood clearance. For the assessment of excretion routes of the tracer, daily urine, and stool collection was made until 8 days in five patients and until 3 days in three patients. Blood and urine samples were counted in an auto gamma counter with corrections made for radioactive decay, background, and count efficacy. Blood and urine concentrations were expressed as % dose per ml and % administered dose, respectively. The activity in the stool was measured in a gamma scintillation counter and expressed as % administered dose.

Parameters for internal radiotherapy of hepatic cancer: Effective half-lives were calculated from the time-activity curves over the visible liver and left middle lung generated

from the ROI counts in the serial planar digital images and over the tumor and AHT from the ROI counts in the serial SPECT images. The effective half-life for the whole body was calculated from the data on excretion of the activity by urine.

In order to estimate the selective accumulation of the tracer in the tumor, the following count ratios were calculated from the ROI counts in the SPECT images: (a) Tumor/AHT count ratio = the mean counts per pixel in the ROI over the tumor/ the mean counts per pixel in the ROI over the AHT; (b) Tumor/lung count ratio = the mean counts per pixel in the ROI over the tumor/the mean counts per pixel in the ROI over the lung, and (c) Lung/AHT count ratio = the mean counts per pixel in the ROI over the lung/the mean counts per pixel in the ROI over the AHT. The ROIs used for calculation of these ratios were the same as those used for obtaining the daily time-activity relationships over the tumor and AHT. The ROI (25 pixels) for the lung was set on the SPECT image through the left middle lung.

An experimental study was performed to estimate the difference in concentration between the tumor and AHT by using the tumor/AHT count ratio. The liver and body phantoms were the same as those used in the experimental study detailed above. A spherical tumor phantom 3.6 cm in diameter and 25 ml in volume was used because the tumors ranged from 3.0 to 4.0 cm in diameter in Patients 1–3. In addition, a small tumor phantom 2.7 cm in diameter and 10 ml in volume was also available. Concentrations of ^{131}I solution for the tumor phantoms were as follows; 0.25, 0.46, 0.99, 5.1, 9.4, and 13.5 μCi/ml. Iodine-131 concentration in the hepatic phantom was fixed at 0.25 μCi/ml. On each occasion the large and small tumor phantoms were fixed into the mid-superior and mid-inferior portions in the liver phantom respectively, it was fixed into the body phantom filled with water. The SPECT data collection, reconstruction, selection of the SPECT image and setting of the ROIs over the tumor and AHT were the same as those which had been employed in the human studies. The relation of tumor/AHT concentration ratio (Y) with tumor/AHT count ratio (X) were as follows: $Y = 7.6\ (X - 0.93)$ ($r = 0.9998$) for the large tumor phantom; and $Y = 11.9\ (X - 0.74)$ ($r = 0.9982$) for the small tumor phantom. The formula for the large tumor phantom was applied for estimation of tumor/AHT concentration ratios in Patients 1–3 because of the similarity in volume between the large tumor phantom and the tumors in these patients.

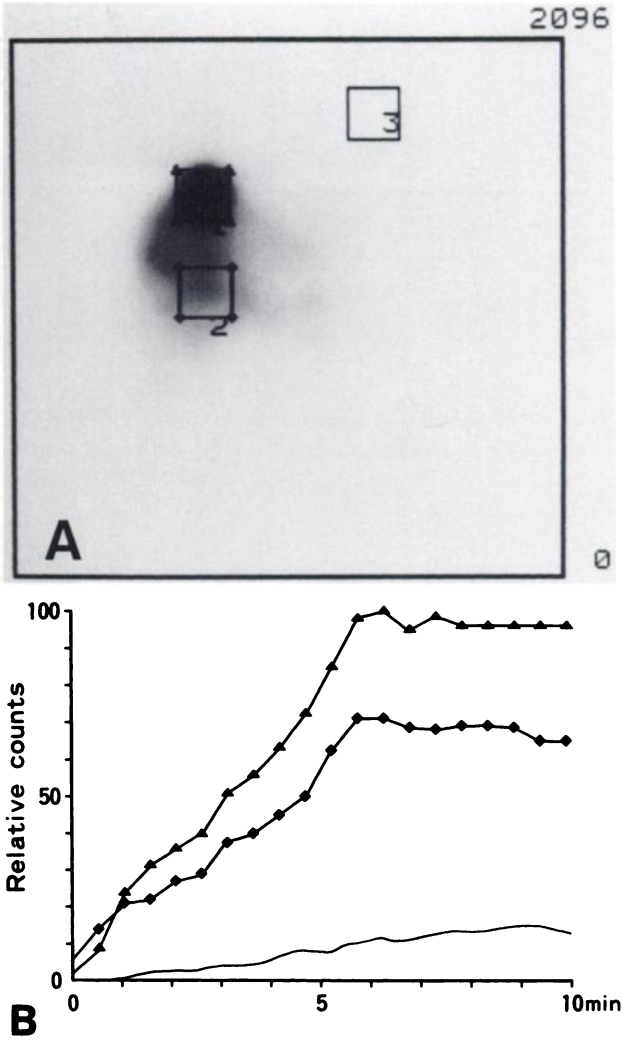

FIGURE 1
Time-activity curves over the tumor, adjacent hepatic tissue (AHT) and lung of Patient 1 during the initial 10 min of [^{131}I]lipiodol infusion. A: ROIs set over the tumor (1), AHT (2), and lung (3). B: A gradual increase in activity was observed over the tumor (top), AHT (middle) and lung (bottom) followed plateaus of activity.

RESULTS

In Vivo Kinetics

Iodine-131 lipiodol accumulated gradually in the liver as the infusion proceeded. Plateaus of the activity were observed almost simultaneously over the tumor, AHT, and lungs from completion of the tracer infusion to 10 min as shown in Figure 1. The activity was higher in four hepatomas with hyperneovascularity and tumor stain and lower in a cholangiocarcinoma with little vascularity than in the AHT. Throughout the imaging sequence, the only organs visualized were the liver and lungs as shown in Figure 2. Neither any of the other organs nor the body silhouette was visualized.

Daily time-activity relationships of iodine-131 lipiodol over the liver and left middle lung is shown in Figure 3. There appear to be two types of time-activity relationships between the liver and lungs.

1. When the activity of the liver showed a rapid decrease for 30 min to Day 1 with a subsequent slow steady state decrease, the pulmonary activity showed an inverse increase having a peak at Day 1 (Patients 3 and 4) or a slower decrease compared to the subsequent steady state decrease (Patient 1).

2. When the hepatic activity showed a linear decrease from the beginning, the pulmonary activity showed an almost linear decrease as well (Patients 2 and 5).

Figure 4 shows daily time-activity relationships over the tumor and AHT. The activity over the tumor

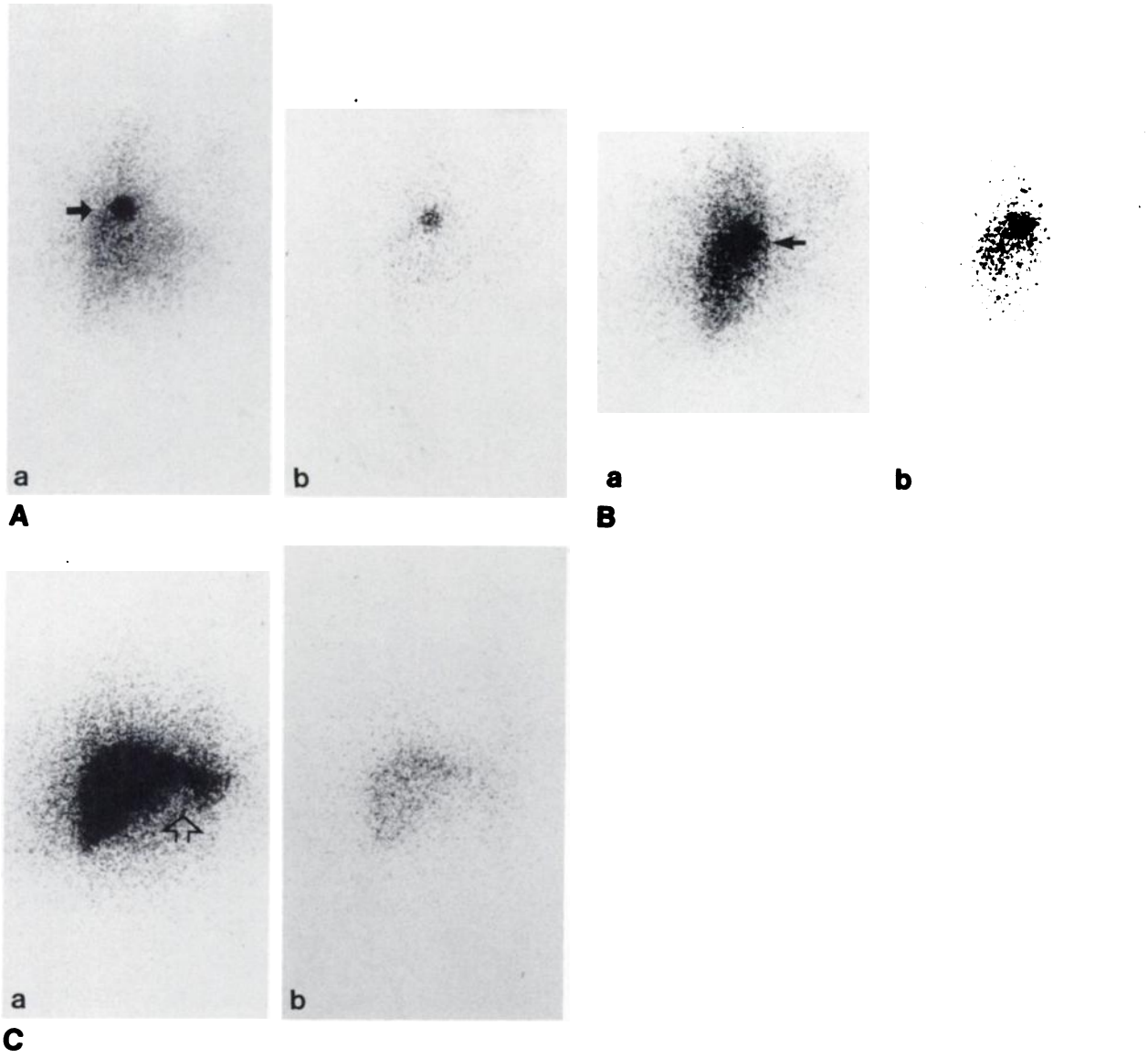

FIGURE 2
Whole-body images of Patients 1 (A), 3 (B), and 5 (C) obtained at 1 hr (a) and 8 days (b) after infusion of [^{131}I]lipiodol. The organs visualized were only the liver and lungs. Intense accumulation of [^{131}I]lipiodol was shown in hepatomas (solid arrows) of Patients 1 and 3, while the cholangiocarcinoma in Patient 5 was delineated as a photon deficient area (open arrow).

decreased rapidly from 2 hr to Day 1 followed by a linear steady state decrease in Patients 1–4, whereas the activity over the AHT in all patients and over the tumor in Patient 5 showed a linear steady state decrease from the beginning.

Figure 5 shows the venous blood concentrations of activity from [^{131}I]lipiodol as a function of time in each patient. The levels were extremely low, an order of 10^{-4}% dose/ml throughout 8 days. The blood concentration increased gradually from 5 min and reached a peak at 2–6 days. From the beginning, it is much higher in Patient 4 than in the other four patients probably due to much larger arterio-venous shunting.

Figure 6 shows the daily and cumulative excretion rate of the activity from [^{131}I]lipiodol in urine as a function of time. The daily excretion rate expressed as % administered dose was relatively constant throughout the 8 days, showing a minimal value of 4.3 ± 2.3% at 1 day and a maximal value of 7.1 ± 2.1% at 4 days. The excretion of activity into stool was extremely low, ranging from 0.01 to 0.1% administered dose for 3 days in three patients in whom this was measured.

Summing up the results mentioned above, we can conclude the following in vivo kinetics of [^{131}I]lipiodol administered via the hepatic artery of patients with vascular cancer of the liver. Iodine-131 lipiodol flows into the hepatic artery by the catheter wedged in place and appears to embolize the hepatic tumor and tissue

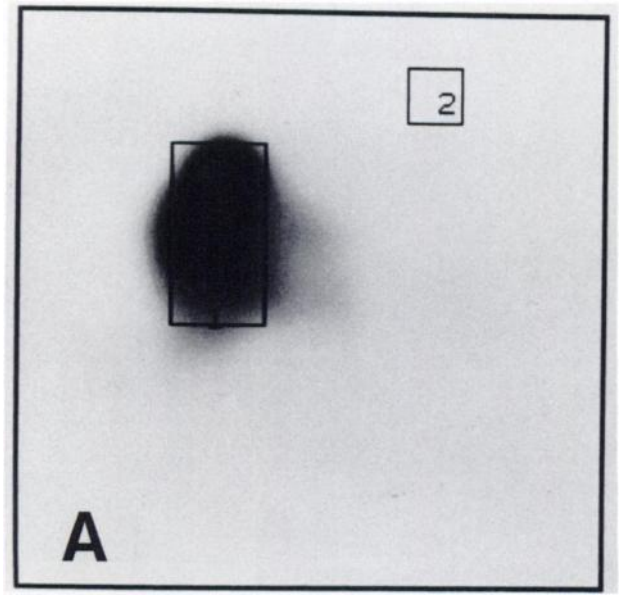

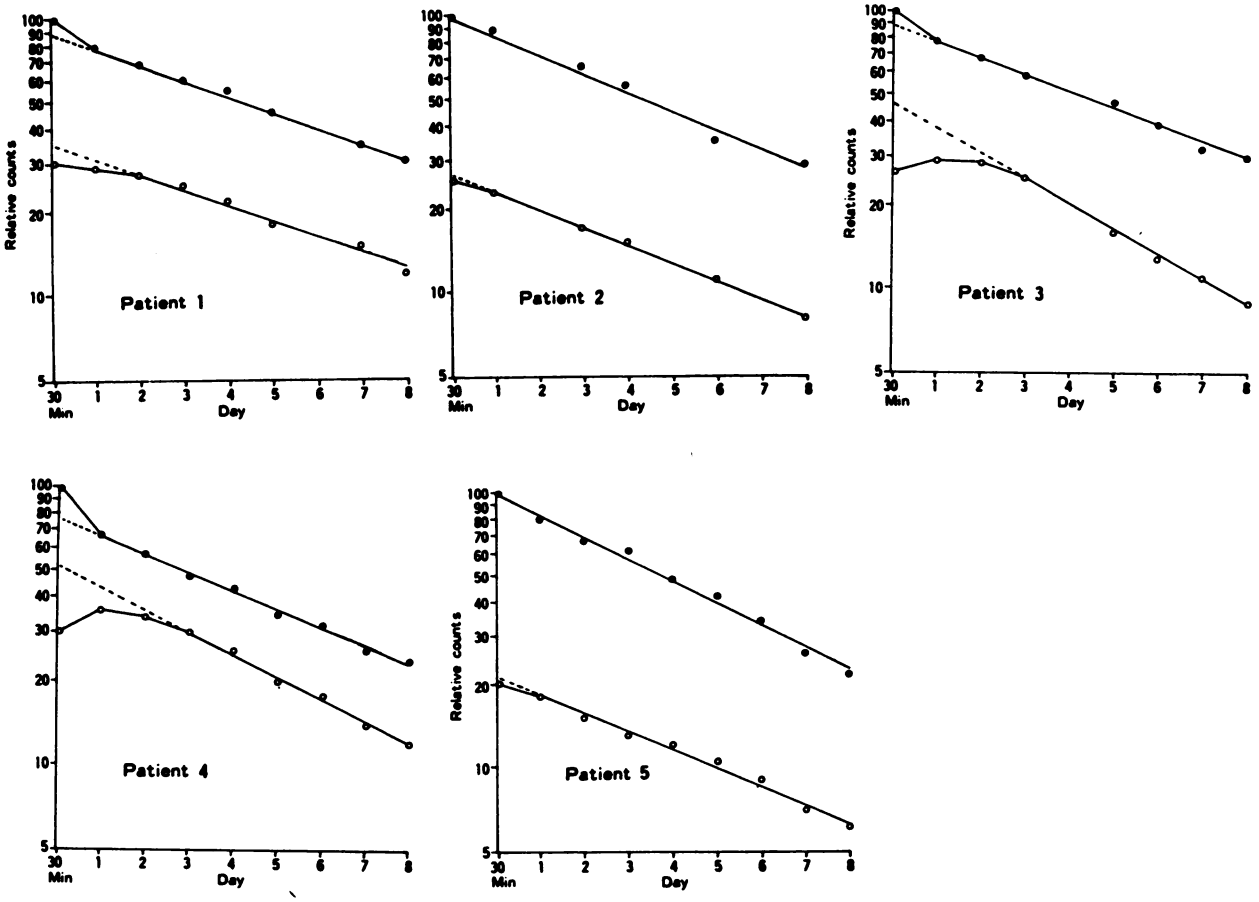

FIGURE 3
A: ROIs set over the liver (1) and lung (2) in the planar digital image to obtain the daily time-activity relationships over them. B: Daily time-activity relationships of [^{131}I]lipiodol over the liver (●) and lung (○).

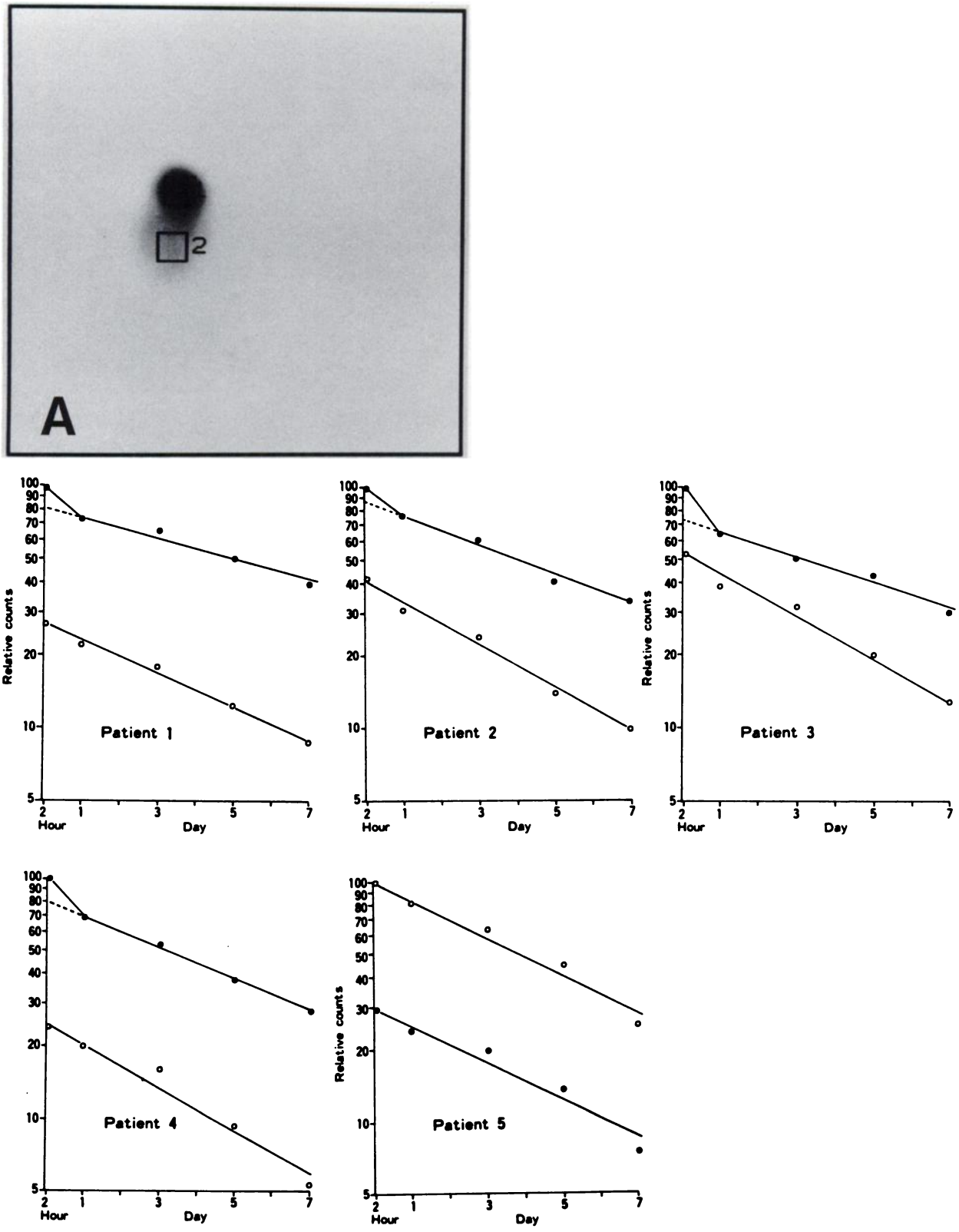

FIGURE 4
A: ROIs set over the tumor (1) and adjacent hepatic tissue (AHT) (2) in the SPECT image to obtain the daily time-activity relationships over them. B: Daily time-activity relationships of [^{131}I]lipiodol over the tumor (●) and AHT (○).

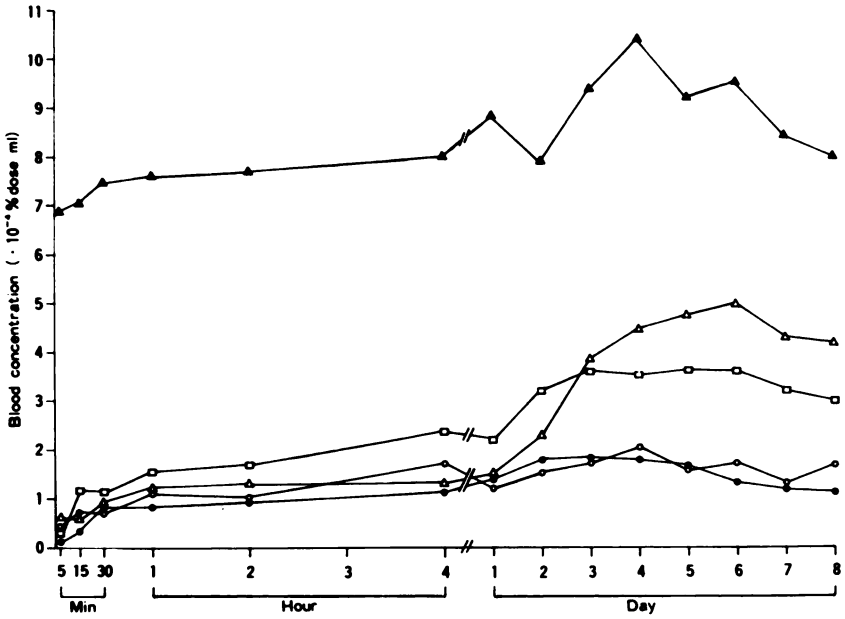

FIGURE 5
The venous blood concentrations of the activity from [^{131}I]lipiodol as a function of time in Patients 1 (○), 2 (●), 3 (△), 4 (▲) and 5 (□).

supplied by the artery. The tumor receives a greater amount of [^{131}I]lipiodol than the AHT. This is followed by secondary embolization in the lungs. Subsequently almost all the activity is excreted into urine. There are at least two components in the hepatic vascular cancer: one rapid and the other slow, while the AHT has only one component.

Parameters for Internal Radiotherapy of Hepatic Cancer

Table 2 shows difference between the initial activity and activity extrapolated to the initial time for the steady state decrease in Figures 3B and 4B. The rapidly decreasing component (rapid component) in the liver was variable, ranging from 0 to 24% and corresponded fairly well to the gradually increasing component in the lungs in each patient. The rapid component in the tumor was also variable, ranging from 0 to 27%. The tumor accumulating tracer had a rapid component whose value ranged from 14 to 27% (mean ± s.d.: 20 ± 5.4%), while the photon deficient (hypovascular) tumor in Patient 5 has no such rapid component.

Table 3 shows effective half-lives ($T_{\frac{1}{2}}$s) of the visible liver, tumor, lungs, and whole body. The $T_{\frac{1}{2}}$ for the activity at the initial 30 min or 2 hr had apparently no difference between the visible liver (mean ± s.d.: 3.9 ± 0.7 days), tumor (3.8 ± 0.7 days), and AHT (3.7 ± 0.6 days) due to the rapid component of the tumor in Patients 1–4. However, the $T_{\frac{1}{2}}$ was longer in the slow component of the tumor (5.7 ± 1.2 days) than in the AHT (3.7 ± 0.6 days). In the lungs, the $T_{\frac{1}{2}}$ was longer for the activity at 30 min (6.1 ± 0.8 days) than for the steady-state decrease (4.3 ± 0.8 days) due to the gradually increasing component in the lungs of Patients 1–4. The $T_{\frac{1}{2}}$ of the whole body ranged from 3.7 to 4.8 days in all patients.

Table 4 shows tumor/AHT, tumor/lung and lung/AHT count ratios. The tumor/AHT count ratio varied from patient to patient. It showed the lowest value at 1 or 3 days and gradually increased afterwards in Patients 1–4. The tumor/AHT concentration ratio was very high, ranging from 7.5 to 21 at 2 hr in Patients 1–3. The tumor/lung count ratio was higher than the tumor/AHT count ratio in Patients 1–3 and 5 throughout the imaging sequence, suggesting the radiation dose was smaller in the lungs than in the AHT. This is also supported by the lung/AHT count ratio.

Slight fever was transiently noted in three of five patients during a week after infusion of the tracer.

DISCUSSION

Transcatheter infusion of lipiodol via the hepatic artery has been increasingly used for the detection and treatment of hepatic cancers in Japan (*2–6*). Even tiny malignant nodules were detected by this method (*3*). The therapeutic effect of lipiodol-chemotherapeutic mixtures on the hepatic cancers appears to be excellent (*5,6*). No noticeable complications arising from these diagnostic and therapeutic methods were reported (*5*). However, its biodistribution and in vivo kinetics in man have not been fully elucidated.

The present study using radioactive lipiodol suggests the following biodistribution and in vivo kinetics of lipiodol when infused into the hepatic artery: (a) the major sites of lipiodol accumulation are the vascular cancer and AHT supplied by the infused artery and the lungs; (b) the vascular cancer has at least two decreasing components for lipiodol retention: one rapid and the other slow; (c) the washout of lipiodol in the slowly decreasing component (slow component) of the tumor

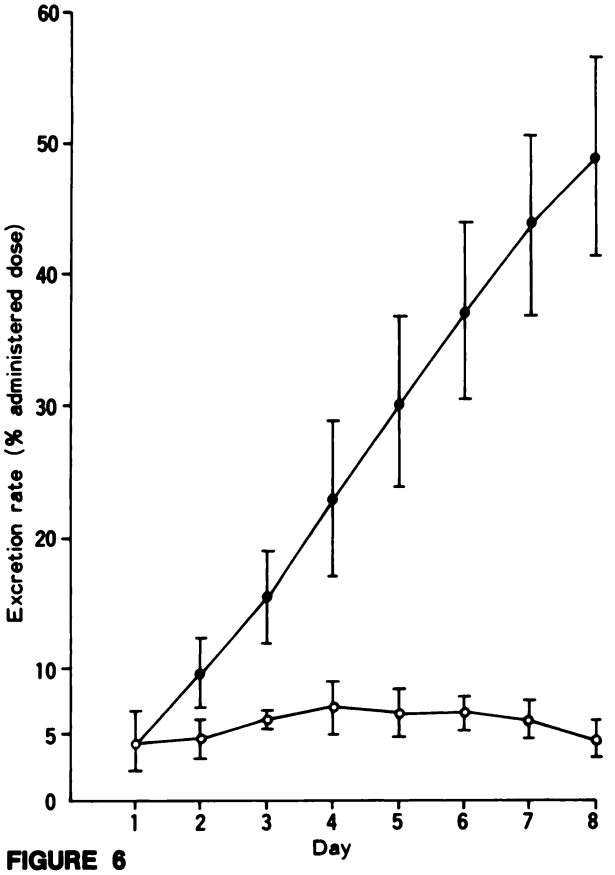

FIGURE 6
The daily (○) and cumulative (●) excretion rate of the activity from [^{131}I]lipiodol into urine as a function of time. Bars show s.d.

is slower than in the AHT; and (d) The major pathway of excretion of lipiodol appears to be as follows; liver including the tumor and AHT ⇒ hepatic veins ⇒ inferior vena cava ⇒ lungs ⇒ aorta ⇒ renal artery ⇒ kidney ⇒ urine.

The rapid component may be due to A-V shunts which may not exist in the AHT and avascular tumor. The effective half-lives shown in Table 3 give the biologic half-lives for the slow component of the tumor and AHT (Table 5). They range from 11 to 83 days in the tumor and from 5.6 to 10 days in the AHT in four patients with hepatoma, this being 1.8 to 8.3 times longer in the tumor than in the AHT. The high tumor/AHT count ratio and difference in clearance of lipiodol between the tumor and AHT further confirm the selective retention of lipiodol observed qualitatively in the plain x-ray films, angiograms and TCT images (*1–6*). The site(s) of selective retention of lipiodol within the tumor are unknown. However, it is suggested that neoplastic vessels may be the major sites of retention (*2*). The tumors showing intense accumulation of [^{131}I] lipiodol in the present study had also angiographic evidence of neovascularity and tumor stain.

The internal radiotherapy of hepatic cancer by intra-

TABLE 2
Difference in Relative Activity between Initial Value and Value Extrapolated to the Initial Time from Steady State Decrease

Patient no.	Difference in relative activity (%)		
	Visible liver	Lung	Tumor
1	12	−5	18
2	0	−2	14
3	14	−20	27
4	24	−22	20
5	0	−1	0
Mean*	13 ± 9.8	−(12 ± 10)	20 ± 5.4

* Mean value of Patients 1–4.

arterial administration of radioactive particle (^{90}Y microspheres) was reported about two decades ago (*8*). Iodine-131 lipiodol might be also a therapeutic radioactive agent for intra-arterial use for the following reasons.

1. Iodine-131 is an acceptable radionuclide for internal radiotherapy as employed in the treatment of hyperthyroidism and thyroid cancer.
2. The effective half-life for the vascular tumors is long enough (5.7 ± 1.2 days) and is longer than those for the AHT (3.7 ± 0.6 days) and lungs (4.3 ± 0.8 days).
3. Tumor/nontumor (AHT and/or lung) ratio is high.
4. The activity in the organs other than the liver and lungs is negligible as shown in the whole-body images and the venous blood concentrations of activity.

The present study suggests that the AHT and lungs are the critical sites for the potential radiation hazards. Therefore, before attempting the internal radiotherapy of hepatoma by this method, the "safe" radiation doses to the AHT and lungs should first be considered. The "safe" radiation doses to the liver and lungs with internally administered radionuclide are not known. However, Levine et al. (*9*) reported that histologic evidence of liver necrosis was found only after 120 Gy in dogs injected with colloidal potassium-32 (^{32}P) chromic phosphate. There were no significant alterations in liver functions below this level. Mantravadi et al. (*10*) used ^{32}P chromic phosphate administered through the superior mesenteric artery to prevent postoperative liver metastases in high risk colorectal cancer patients. The dose to the entire liver was ~30 Gy and only transient elevation of serum LDH and GOT in two out of eight patients was observed as of 5 mo after treatment. Tolerance of the entire liver to external irradiation has been estimated to be 30 Gy, with radiation hepatitis developing when this level is exceeded (*11*). Whole-lung tolerance doses to external irradiation would appear to be 18 Gy in ten fractions or 25 Gy in 20 fractions,

TABLE 3
Effective Half-Lives (Days) of the Visible Liver, Tumor, Adjacent Hepatic Tissue (AHT), Lung, and Whole Body

Patient no.	Visible liver		Tumor		AHT	Lung		Whole body
	T_1*	T_2†	T_1	T_2	T_1=T_2	T_1	T_2	
1	4.2	5.1	5.0	7.3	4.5	6.5	5.4	4.8
2	4.3	4.3	4.0	5.2	3.3	5.0	4.5	3.7
3	4.1	5.2	3.2	5.7	3.4	6.1	3.7	4.2
4	2.8	4.6	3.1	4.6	3.5	6.7	3.7	4.3
5	3.7	3.7	3.8	3.8	3.7	4.9	4.6	4.0
Mean‡	3.9 ± 0.7	4.8 ± 0.4	3.8 ± 0.9	5.7 ± 1.2	3.7 ± 0.6	6.1 ± 0.8	4.3 ± 0.8	4.3 ± 0.5

* $T_{1/2}$ for the activity at initial 30 min or 2 hr.
† $T_{1/2}$ of the steady state decrease.
‡ Mean effective half-life of Patients 1–4.

however, the doses decrease to 11 Gy in ten fractions and 15 Gy in 15 fractions when actinomycin D is given either before, during or after irradiation (*12*). Patients receiving lung radiation doses of up to 15 Gy due to spillover of iodine-131-labeled oily contrast medium in internal endolymphatic therapy did not show any visible changes on the chest x-ray films (*13*). Therefore reasonable guidelines for the "safe" doses would appear to be 30 Gy to the entire liver and 11 Gy to the whole lungs respectively, when the lowest values from these reports are employed.

We would like to consider the therapeutic potential of this agent in the present five cases on the basis of the data available in this study. Patient 5 is not the candidate for this internal radiotherapy, because the activity within the tumor is lower than that within the AHT. The other four patients have the tumors which accumulated [^{131}I]lipiodol. To calculate the mean absorbed doses to the tumor, AHT and lungs, the following assumptions are made:

1. The activity within the tumor, AHT and lungs is uniformly distributed.
2. The lung/AHT count ratio is the concentration ratio.
3. The weight of the tumor is 16 g in Patient 1, 22 g in Patient 2, 24 g in Patient 3 and 850 g in Patient 4, this being estimated from the spherical volume calculated from the average diameter in the CT images (Table

TABLE 4
Tumor/Adjacent Hepatic Tissue (AHT), Tumor/Lung and Lung/AHT Count Ratios

Ratio	Patient no.	Time				
		2 hr	1 day	3 days	5 days	7 days
Tumor/AHT	1	3.7 (21)*	3.3 (18)	3.6 (21)	4.1 (24)	4.5 (27)
	2	2.4 (11)	2.4 (11)	2.5 (12)	2.8 (14)	3.3 (18)
	3	1.9 (7.5)	1.7 (6.0)	1.6 (5.3)	2.1 (9.1)	2.3 (11)
	4	4.1	3.5	3.4	4.0	5.4
	5	0.29	0.30	0.30	0.29	0.28
Tumor/lung	1	9.7	8.7	8.8	10.8	11.5
	2	12.0	10.0	9.3	9.0	11.4
	3	6.8	4.0	3.9	5.3	5.5
	4	3.7	2.5	2.3	2.5	2.7
	5	2.4	2.7	2.7	2.6	2.2
Lung/AHT	1	0.38	0.38	0.41	0.38	0.39
	2	0.20	0.24	0.27	0.31	0.29
	3	0.28	0.43	0.41	0.40	0.42
	4	1.1	1.4	1.5	1.6	2.0
	5	0.12	0.11	0.11	0.11	0.13

* Tumor/AHT concentration ratio obtained by use of the formula; $y = 7.6 (X - 0.93)$.

TABLE 5
Biologic Half-Lives of the Slow Component of the Tumor and Adjacent Hepatic Tissue (AHT) and Its Tumor/AHT Ratio

Patient no.	Biologic half life (days)		Tumor/AHT ratio
	Tumor	AHT	
1	83	10	8.3
2	15	5.6	2.7
3	19	5.9	3.2
4	11	6.2	1.8
5	7.2	6.9	1.0

1). The AHT weight is 1,000 g in Patients 1, 3, and 4 who received [^{131}I]lipiodol via the RHA or LHA and 1809 g (*14*) in Patient 2 in whom the catheter tip was wedged in the PHA.

4. To calculate accurately the absorbed doses to the tumor, AHT and lungs, the doses from nearby tissues must be considered in addition to the self-dose. In this calculation, however, only the self-doses are considered because the penetrating radiation doses to the tumor, AHT, and lungs from nearby tissues cannot be calculated from the MIRD tables and is much smaller when compared to the self-doses (*15*).

5. The interpolated "S" values for ^{131}I are used to calculate the self-doses to the tumor and AHT. The following equation is generated by using ^{131}I organ self-irradiation "S" values and organ weights in MIRD pamphlets (*14*): $\log S\ (\text{rad}/\mu\text{C}\cdot\text{hr}) = -0.937 \times \log \text{mass}\ (\text{g}) - 0.494$ ($r = 0.9976$), (mass 8.3 to 69,880 g). From this equation, the interpolated "S" values are 2.4×10^{-2}, 1.8×10^{-2}, 1.6×10^{-2}, 5.8×10^{-4}, 5.0×10^{-4} rad/μCi·hr for 16, 22, 24, 850 g tumors and 1,000 g AHT, respectively. The "S" value for the AHT in Patient 2 is 3.0×10^{-4} rad/μCi·hr, the value for liver self-irradiation in the MIRD table. The "S" value, 4.5×10^{-4} rad/μCi·hr from the MIRD table is used for lung self-irradiation.

6. The tumors had rapid and slow components. Although the effective half-life for the slow component is available as T_2 in Table 3, more frequent measurements would have been needed to obtain that for the rapid component within 24 hr. Therefore, the cumulated activity originated from the rapid component is assumed to be the triangular area enclosed by the solid and dotted lines in Figure 4B.

7. The lung cumulated activity during the period before the steady state decrease is estimated from the time-activity curve in Figure 3B.

From these assumptions, the following equations to calculate the self-dose (Gy) can be derived.

$D_{tumor} = S_t(\tilde{A}_1 + \tilde{A}_2) \times 10^{-2}$ ----- (1), where S_t is the interpolated "S" value for the individual tumor

TABLE 6
Summary of Values Concerning Dosimetry

Patient no.	Case*	Tumor			AHT			Lungs			Total initial activity (mCi)	Ratios of absorbed dose	
		D	Ã	A	D	Ã	A	D	Ã	A		Tumor/AHT	Tumor/lung
1	a	100	417	2.0	4.6	921	5.9	2.1	465	2.3	10.2	22	48
	b	652	2719	13.0	30.0	6005	38.5	13.6	3032	14.7	66.2		
	c	526	2193	10.5	24.2	4844	31.0	11.0	2446	11.8	53.3		
	d	295	1230	5.9	13.6	2717	17.4	6.2	1372	6.8	30.1		
2	a	100	556	3.6	9.1	3034	26.6	2.2	490	3.0	33.2	11	45
	b	330	1835	11.7	30.0	10012	87.8	7.3	1617	9.7	109.2		
	c	500	2780	17.8	45.5	15170	133.0	11.0	2450	14.8	165.6		
	d	90	500	3.3	8.2	2742	24.0	2.0	443	2.7	30.0		
3	a	100	625	4.3	13.9	2773	23.6	5.9	1308	6.6	34.5	7.2	17
	b	216	1350	9.3	30.0	5990	51.0	12.7	2825	14.3	74.6		
	c	186	1163	7.9	25.9	5176	43.9	11.0	2433	12.3	64.1		
	d	87	544	3.7	12.1	2412	20.5	5.1	1138	5.7	29.9		
4	a	100	17237	133.0	23.0	4603	38.1	39.2	8718	41.9	213.0	4.3	2.6
	b	130	22408	173.5	30.0	5984	49.6	50.7	11333	54.5	277.6		
	c	28	4861	37.5	6.5	1293	10.7	11.0	2450	11.8	60.0		
	d	14	2430	18.8	3.2	649	5.4	5.5	1229	5.9	30.1		

*In case of tumor dose, 100 Gy (a); AHT dose, 30 Gy (b); lung dose, 11 Gy (c); or infusion dose of activity, 30 mCi (d). D: Self-absorbed dose (Gy); Ã: Cumulated activity ($\times 10^3$ μCi·hr); A: Initial activity (mCi).

mass, $\tilde{A}_1$ is the cumulated activity in the rapid component, 1,000 μCi × 24 hr × ½ × A_1, and $\tilde{A}_2$ is the cumulated activity in the slow component, 1.44 × 1,000 μCi × 24 hr × A_2 × T_2. A_1 (mCi) is the initial activity in the rapid component and A_2 is that in the slow component in the tumor. T_2 (days) is the effective half-life for the slow component in the tumor.

Similarly, $D_{AHT} = S_{AHT}\tilde{A} \times 10^{-2}$ ----- (2), where S_{AHT} is the "S" value for the AHT, $\tilde{A}$ is the cumulated activity in the AHT, 1.44 × 1,000 μCi × 24 hr × AXT_1. A (mCi) is the initial activity in the AHT and T_1 (days) is the effective half-life for the AHT.

$D_{lungs} = S_{lungs}(\tilde{A}_1 + \tilde{A}_2) \times 10^{-2}$ ----- (3), where S_{lungs} is the lung self-irradiation "S" value, $\tilde{A}_1$ is the cumulated activity in the lungs during the period before the steady state decrease and $\tilde{A}_2$ is the cumulated activity in the lungs during the steady state decrease, 1.44 × 1,000 μCi × 24 hr × A_2 × T_2. A_2 (mCi) is the activity at the day when the steady state decrease begins (Fig. 3B). T_2 (days) is the effective half-life for the steady state decrease.

From these equations and data in the present study, we can estimate the self-doses to the tumor, AHT, and lungs, the initial activity in them and finally the activity to be infused. If the desired self-dose to the tumor is determined, the dose of activity in the tumor can be calculated from Eq. (1), where the relative ratio of A_1 to A_2 can be derived from the values in Table 2. The initial dose of activity in the AHT and lungs in this situation can be determined by using the Tumor/AHT concentration ratio and Lung/AHT count ratio at 2 hr in Table 4. In Patient 4, Tumor/AHT count ratio is assumed to be the concentration ratio. Then the self-doses to the AHT and lungs can be calculated from Eqs. (2) and (3), respectively. Table 6 summarizes the values concerning dosimetry calculated by the above-mentioned method in a variety of cases.

For example, if one wants to deliver 100 Gy to the tumor (Table 6, a lines), the doses of activity in the tumor would be 2.0, 3.6, 4.3, and 133 mCi in Patients 1–4, respectively. In this situation, the initial doses of activity in the AHT would be 5.9, 26.6, 23.6 and 38.1 mCi which would deliver 4.6, 9.1, 13.9, and 23 Gy to the AHT in Patients 1–4, respectively. The initial doses of activity in the lungs would be 2.3, 3.0, 6.6, and 41.9 mCi which would deliver 2.1, 2.2, 5.9 and 39.2 Gy to the lungs in Patients 1–4, respectively. Then the total doses of activity to be infused to deliver 100 Gy to the tumor would be 10.2, 33.2, 34.5, and 213 mCi in Patients 1–4, respectively.

Thus, the therapeutic benefit is expected without significant radiation hazards to the AHT and lungs in Patients 1–3. However, Patient 4 would suffer from radiation pneumonitis at the tumor dose of 100 Gy. From the "safe" dose consideration mentioned above, Patient 4 may not be the candidate for this internal radiotherapy, because the tumor dose would be below 28 Gy, when the radiation dose to the lungs is kept below the "safe" dose, 11 Gy (Table 6, Patient 4, c line). In this connection, if Patients 1–3 receive the "safe" dose to the AHT or lungs, the following doses can be calculated (Table 6, Patients 1–3, b or c lines): When Patients 1 and 3 receive lung "safe" dose, 11 Gy, the doses to the tumor and AHT are 526 and 24.2 Gy in Patient 1 and 186 and 25.9 Gy in Patient 3. When the AHT dose is 30 Gy in Patient 2, the doses to the tumor and lungs are 330 and 7.3 Gy, respectively. In these situations, the doses of activity to be infused would be 53.3, 109.2, and 64.1 mCi in Patients 1–3, respectively.

An adverse factor for the treatment of hepatic cancer suggested by the present study is shunting from the tumor to the lungs. Hepatic arterial infusion using technetium-99m macroaggregated albumin (MAA) may be one of the methods to estimate the degree of this shunting (*16*). From the clinical point of view, it may be necessary to estimate the general safe dose of activity to be infused so as to avoid the potential radiation hazards to the AHT and lungs. When the catheter tip is wedged in the PHA, RHA or LHA, [^{131}I]lipiodol will distribute to the whole liver and nearly half of the liver, respectively. Assuming that the "safe" radiation dose is 30 Gy for the liver and 11 Gy for the lungs, the effective half-life is 3.7 days in the liver and 4.3 days in the lung (the mean values in the present study) and that the activity decreases exponentially from the beginning, the "safe" activity would be 78 mCi in the whole liver, 47 mCi in the half of the liver and 16 mCi in the whole lungs. Therefore the activity in the whole lungs appears to be the limiting dose to define the "safe" activity to be infused. The total activity in the liver and lungs at 30 min can be regarded as equal to the injected dose because the other organs were not visualized and the blood concentrations were extremely low. When the % of injected dose in the lungs at 30 min was estimated by the geometric mean counts over the liver and lungs after background subtraction in the conjugate views in the five cases studied, it ranged from 5% to 36% (mean ± s.d.: 18 ± 12%) and the value extrapolated from the steady state decrease to the initial time ranged from 5.4 to 62% (28 ± 24%). Assuming that the typical extrapolated value is 50%, the "safe" activity to be infused would be 32 mCi, twice of the "save" activity of the lungs. Therefore 30 mCi may be a "safe" infusion dose by a wide margin to initiate a therapeutic trial. For example, if the patients receive infusion doses of 30 mCi, the tumor doses would be 295, 90, and 87 Gy in Patients 1–3, respectively, with the doses to AHT and lungs being far smaller than the "safe" radiation doses (Table 6, Patients 1–3, d lines). We have treated 18 patients with hepatoma by the present method using an infusion dose of <30 mCi. The initial therapeutic results will be reported in the near future.

ACKNOWLEDGMENTS

The authors thank Dr. Hiroshi Ogawa and his staff, Daiichi Radioisotope Laboratories, Ltd., for preparing [^{131}I]lipiodol and Messrs Atsunori Okada and Toyotsugu Kiku for their technical assistance. They also thank Prof. Brahm Shapiro, the University of Michigan Medical Center, Ann Arbor, for correcting the English text.

REFERENCES

1. Nakakuma K, Tashiro S, Uemura K, et al. Studies on anticancer treatment with an oily anticancer drug injected into the ligated hepatic artery for liver cancer (preliminary report) (in Japanese). *Nichidoku Iho* 1979; 24:675–682.
2. Nakakuma K, Tashiro S, Hiraoka T, et al. Hepatocellular carcinoma and metastatic cancer detected by iodized oil. *Radiology* 1985; 154:15–17.
3. Yumoto Y, Jinno K, Tokuyama K, et al. Hepatocellular carcinoma detected by iodized oil. *Radiology* 1985; 154:19–24.
4. Maki S, Konno T, Maeda H. Image enhancement in computerized tomography for sensitive diagnosis of liver cancer and semiquantitation of tumor selective targeting with oily contrast medium. *Cancer* 1985; 56:751–757.
5. Konno T, Maeda H, Iwai K, et al. Effect of arterial administration of high-molecular-weight anticancer agent SMANCS with lipid lymphographic agent on hepatoma: a preliminary report. *Eur J Cancer Clin Oncol* 1983; 19:1053–1065.
6. Ohishi H, Uchida H, Yoshimura H, et al. Hepatocellular carcinoma detected by iodized oil: Use of anticancer agents. *Radiology* 1985; 154:25–29.
7. Contreras MA. Bale WF, Spar IL. Iodine monochloride (ICL) iodination techniques. *Meth Enzymol* 1983; 92:277–292.
8. Ariel IM. Treatment of inoperable primary pancreatic and liver cancer by the intra-arterial administration of radioactive isotopes (Y^{90} radiating microspheres). *Ann Surg* 1965; 162:267–278.
9. Levine B, Hoffman H, Freedlander SO. Distribution and effect of colloidal chromic phosphate (P^{32}) injected into the hepatic artery and portal vein of dogs and man. *Cancer* 1957; 10:164–172.
10. Mantravadi RVP, Spigos DG, Karesh SM, et al. Work in progress: intra-arterial P-32 rectal cancer patients. *Radiology* 1983; 148:555–559.
11. Ingold JA, Reed GB, Kaplan HS, et al. Radiation hepatitis. *Am J Roentgenol* 1965; 93:200–208.
12. Margolis LW, Phillips TL. Whole lung irradiation for metastatic tumor. *Radiology* 1969; 93:1173–1179.
13. Weissleder H, Pfannenstiel P, Strickstrock KH, et al. Principles of endolymphatic therapy with radioactive substance. In: *Progress in lymphology II.* Thieme Stuttgart, 1970: 231–233.
14. Snyder WS, Ford MR, Warner GG, et al. "S," absorbed dose per unit cumulated activity for selected radionuclides and organs. MIRD Pamphlet No. 11. New York: Society of Nuclear Medicine, 1975.
15. Leichner PK, Klein JL, Garrison JB, et al. Dosimetry of ^{131}I-labeled anti-ferritin in hepatoma: A model for radioimmunoglobulin dosimetry. *Int J Radiat Oncol Biol Phys* 1981; 7:323–333.
16. Ziessmann HA, Thrall JH, Gyves JW, et al. Quantitative hepatic arterial perfusion scintigraphy and starch microspheres in cancer chemotherapy. *J Nucl Med* 1983; 24:871–875.